INL/RPT-22-68830
Revision 0

INL Contributions to Draft HTTF Benchmark Specifications

August 2022

Robert Kile

Aaron Epiney

INL is a U.S. Department of Energy National Laboratory
operated by Battelle Energy Alliance, LLC

INL/RPT-22-68830
Revision 0

INL Contributions to Draft HTTF Benchmark Specifications

Robert Kile

Aaron Epiney

September 2022

Idaho National Laboratory
Advanced Reactor Technologies
Idaho Falls, Idaho 83415

http://www.art.inl.gov

Prepared for the
U.S. Department of Energy
Office of Nuclear Energy
Under DOE Idaho Operations Office
Contract DE-AC07-05ID14517

Page intentionally left blank

INL ART Program

INL Contributions to Draft HTTF Benchmark Specifications

INL/RPT-22-68830
Revision 0

August 2022

Technical Reviewer: (Confirmation of mathematical accuracy, and correctness of data and appropriateness of assumptions.)

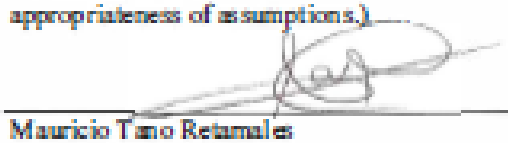

Mauricio Tano Retamales — 08/29/2022
Date

Approved by:

M. Davenport — 8/30/2022
Michael E. Davenport — Date
ART Project Manager

Gerhard Strydom — 08/29/2022
Gerhard Strydom — Date
ART Co-NTD

Michelle Sharp — 8/29/2022
Michelle T. Sharp — Date
INL Quality Assurance

ABSTRACT

The High-Temperature Test Facility (HTTF) is an integral-effects thermal hydraulics test facility at Oregon State University designed as a ¼-length-scale model of the modular high-temperature gas-cooled reactor 350-MW core (mHTGR-350). In the spring and summer of 2019, several experiments were conducted at HTTF providing a valuable source of gas-cooled reactor thermal hydraulics data. Idaho National Laboratory (INL), Oregon State University, Argonne National Laboratory, and Canadian Nuclear Laboratories have partnered to use this experimental data to develop a gas-cooled reactor thermal hydraulics benchmark led by INL under the auspices of the Advanced Reactor Technologies program. This report provides some context on the benchmark, HTTF, and previous Reactor Excursions and Leak Analysis Program 5 3D HTTF modeling. It also provides a draft of the benchmark specifications for the depressurized conduction cooldown problem, which is the INL-led benchmark problem.

Page intentionally left blank

CONTENTS

FIGURES

TABLES

Page intentionally left blank

ACRONYMS

ANL	Argonne National Laboratory
CFD	Computational Fluid Dynamics
CNL	Canadian Nuclear Laboratories
DCC	Depressurized Conduction Cooldown
HTGR	High-Temperature Gas-Cooled Reactors
HTTF	High-Temperature Test Facility
INL	Idaho National Laboratory
mHTGR	Modular High-Temperature Gas-Cooled Reactor
OSU	Oregon State University
PCC	Pressurized Conduction Cooldown
RCCS	reactor cavity cooling system
RCST	Reactor Cavity Storage Tank
RELAP	Reactor Excursions and Leak Analysis Program

Page intentionally left blank

INL Contributions to Draft High-Temperature Test Facility (HTTF) Benchmark Specifications

1. Introduction

The last several years have seen significant interest in the design and deployment of high-temperature gas-cooled reactors (HTGRs). The design and deployment of HTGRs requires modeling and simulation tools capable of predicting HTGR performance during steady state and transients. To assess the capabilities of existing codes for steady-state and transient modeling in HTGRs, experimental data are needed. Additionally, when existing codes provide different answers for the same problem, it is necessary to understand the factors that drive these differences. To that end, it is essential to develop a comprehensive benchmark that includes both code-to-code and code-to-data comparisons for HTGR conditions. Previous HTGR benchmarks have been primarily computational in nature, with little to no validation component.

The HTTF is an electrically heated integral-effects thermal hydraulics test facility at Oregon State University (OSU) designed to provide code validation data for HTGR-relevant conditions. In the spring and summer of 2019, several experiments were performed at HTTF that produced high-quality measured data applicable for an HTGR benchmark. Over the last few years, loose collaborations formed between organizations using the HTTF data for their own modeling and simulation purposes. These organizations include Idaho National Laboratory (INL), OSU, Argonne National Laboratory (ANL), and Canadian Nuclear Laboratories (CNL). This group of collaborators, under INL leadership, got together early in Fiscal Year 2022 and put together a proposal to formalize the collaboration through the development of an HTGR thermal hydraulics benchmark based on HTTF data. In February of 2022, the proposal for an HTTF benchmark was submitted to the Organization for Economic Cooperation and Development – Nuclear Energy Agency (OECD-NEA or OECD) for their consideration and ultimately accepted. In that time, INL—through the Advanced Reactor Technology (ART) program—has led the development of draft benchmark specifications. This milestone report contains a description the HTTF, an overview of the proposed benchmark, and a detailed description of the INL-led contributions to the benchmark specifications.

1.1 HTTF Description

The HTTF is an electrically heated, helium-cooled integral-effects facility designed as a ¼-length-scale model for a block-type gas-cooled reactor design known as the modular high-temperature gas-cooled reactor 350 MW (mHTGR-350). The mHTGR-350 itself is an OECD benchmark for HTGR neutronics and thermal hydraulics [1], but the mHTGR-350 benchmark is both multiphysics and entirely computational in nature. The facility includes a reactor vessel, reactor cavity cooling system (RCCS), a full primary loop, and a secondary loop that includes a steam generator, and a volume known as the reactor cavity storage tank (RCST), which is a volume of helium at atmospheric pressure that serves as a pressure boundary for depressurized conduction cooldown (DCC) experiments [2]. A mock-up of the vessel and RCST is in Figure 1.

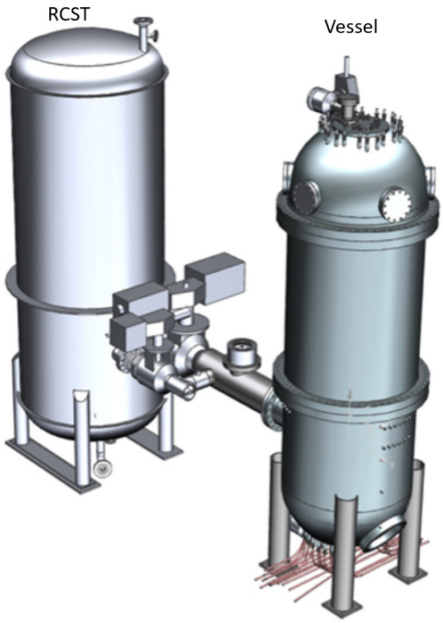

Figure 1. Rendition of HTTF vessel and RCST.

The core of the HTTF is composed of hexagonal blocks of an aluminum-oxide based ceramic. The blocks have holes in them, allowing for primary coolant flow, bypass flow, and room for the 210 graphite resistive heater rods. The heater rods are capable of providing a combined power up to 2.2 MW. The core is an annular configuration, with an inner reflector, rings of heated blocks, and an outer reflector. The core layout can be seen in Figure 2. Coolant flows downward through the core, primarily through the core coolant channels, but a small fraction of coolant flows through the bypass channels.

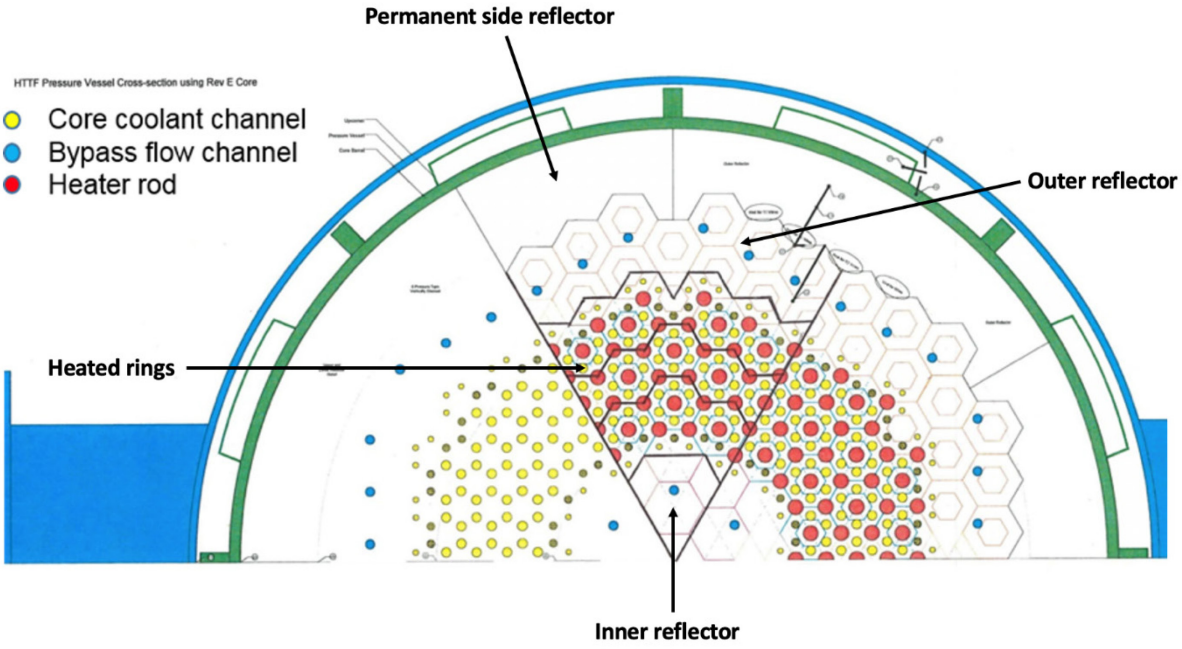

Figure 2. HTTF core layout.

The HTTF operates at a pressure of 0.7 MPa, lower than the 6.39 MPa for the mHTGR-350. Consequently, the blowdown phase of a DCC will not be accurately captured, but the long-term heatup and conduction cooldown will. During the conduction cooldown phase, heat is removed by the RCCS. The HTTF RCCS consists of a set of square panels surrounding the vessel with water flowing from bottom-to-top.

The HTTF contains over 500 instruments, over 400 of which are thermocouples. The high amounts of measured data make the facility an excellent candidate for developing a benchmark. Redundancies were built into the instrumentation plan so that even in the event of instrumentation failure, a similar measurement is still available. The biggest challenge with using HTTF data to define a benchmark is that the HTTF does not include any measurements of the primary coolant flow rate.

1.2 Proposed Benchmark Overview

The mHTGR-350 benchmark is both multiphysics and entirely computational. Consequently, differences in solutions to that benchmark may arise due to differences in neutronics solution, the thermal hydraulics solution, or both. A single-physics benchmark like the HTTF thermal hydraulics benchmark, eliminates the propagation of neutronics errors into thermal hydraulics solutions. A benchmark with experimental data also provides an opportunity to perform validation rather than just code-to-code verification. The proposed HTTF benchmark will be composed of three problems, with each problem having three exercises. Each problem represents different thermal hydraulic conditions from an HTTF experiment, allowing for comparison against measured data. Problems are intended to be solved with systems codes, computational fluid dynamics (CFD) codes, or systems codes coupled to CFD codes. The list of problems, the physical phenomena they are intended to model, and the relevant experiments can be seen in Table 1. Each problem is also divided into three exercises: fixed boundary conditions (code-to-code comparison), open boundary conditions (best-estimate modeling and validation), and error scaling (validation extrapolation).

Table 1. Benchmark problems, where “coupled” refers to coupled systems-code-to-CFD modeling.

Problem	**Physical Phenomena**	**Type of Modeling**	**HTTF Experiment**	**Lead Organization**
1	Lower plenum mixing	CFD	PG-28	OSU
2	DCC transient	Systems code/coupled	PG-29	INL
3	Pressurized conduction cooldown (PCC) transient	Systems code/coupled	PG-27	ANL

The ART program is spearheading the benchmark development and leading the work for problem two. Current benchmark participants include INL, using Reactor Excursions and Leak Analysis Program (RELAP)5-3D for systems-code modeling, ANL using the Systems Analysis Module for systems-code modeling, OSU focusing on CFD modeling with systems-code conditions provided by INL, and CNL with RELAP5-3D and their own in-house tool called ARIANT.

2. RELAP5-3D Modeling of the HTTF

The RELAP5-3D modeling for this benchmark descends from a RELAP5-3D model developed at INL that meets Nuclear Quality Assurance standards [3]. The Nuclear Quality Assurance model was modified with relevant time-dependent boundary conditions to re-create HTTF experiments using techniques developed for RELAP5-3D modeling of the HTTF test PG-26 during Fiscal Year 2020 [4]. For Exercise 1 (fixed boundary conditions, code-to-code comparison) of problems one and two, a simplified model that included only the core, vessel, and RCCS is used. The emissivities of some of the materials were modified from those in the Bayless model [3]. These revised values can be seen in Table 2. The RELAP5-3D model includes a cavity between the core vessel and the RCCS. This cavity is thermally coupled to both the outside of the reactor vessel and the inside of the RCCS cavity.

Table 2: Revised emissivities.

Material	Emissivity (-)
Graphite heater rods	0.9
Core ceramic blocks	0.581
Shot Tech SiC 80 (permanent side reflector)	0.581
Stainless steel for reactor pressure vessel and barrel	0.25
RCCS panel stainless steel	0.074

3. Benchmark Specifications for Problem Two

Problem two models a DCC transient. In an HTGR, this occurs when the coolant pressure boundary is ruptured and helium escapes to containment. In HTTF, this occurs when valves connecting the vessel to the RCST are opened. The DCC portion of the benchmark is based on the PG-29 experiment conducted from July 24–26, 2019. The experiment started on July 24, 2019 at 9:15:42 pm following the completion of HTTF experiment PG-28 [5]. The initial conditions selected to define the benchmark were taken from the measured data on July 24 at 3:42:20 pm because this time provides an opportunity to model the entire heatup and a period of approximately four hours prior to heatup, during which time the pump speed (and correspondingly the coolant flow rate) was relatively constant. Starting the modeling at the time the PG-29 experiment began would mean a much larger fraction of the heatup period used a variable pump speed.

3.1 Exercise One: Fixed Boundary Conditions (Code-to-Code Comparison)

The code-to-code comparison is composed of three sub-exercises. The first is a full-power steady state. The second sub-exercise is a DCC from the full-power steady state. This allows for relatively simply boundary conditions and uses the Exercise 1A (full-power steady-state) solution as the initial conditions. The third sub-exercise uses PG-29-like conditions. Initial conditions for this sub-exercise are based on measured HTTF values from July 24, 2019 at 3:42:20 pm. The boundary conditions for this sub-exercise are the most complex but are derived directly from the measured data.

In all cases, the axial power distribution in HTTF is uniform due to the use of resistive heating rather than fission heating

3.1.1 Exercise 1A: Full-Power Steady State

HTTF was never run at full-power steady state, but this simple case provides an opportunity to assess steady-state solution techniques between systems codes and provides a set of initial conditions for Exercise 1B without the need to rigorously define temperatures at many locations throughout the core. The relevant boundary conditions can be seen in Table 3. The measured thermophysical properties of the core ceramic, as reported in the HTTF design description should be used for this problem [2]. If temperatures should exceed the highest measured temperature, the value of thermal conductivity or volumetric heat capacity at the highest temperature should be used. If temperatures should fall below the lowest measured temperature, the thermal conductivity or volumetric heat capacity from the lowest temperature should be used. The 2.2 MW is distributed evenly among the 10 heater rods, and as stated earlier, the axial power distribution is uniform. This problem should be solved using steady-state solution techniques if available.

Table 3. Full-power steady state boundary conditions.

Parameter	Value
Power (MW)	2.2
Helium Inlet Temperature (K)	500.0
Helium Flow Rate (kg/s)	1.0
Helium Pressure (MPa)	0.7
RCCS Water Inlet Temperature (K)	313.2
RCCS Water Flow Rate (K)	1.0
RCCS Water Pressure (MPa)	0.1
RCCS cavity air inlet temperature (K)	300.0
RCCS cavity air flow rate (kg/s)	0.025

3.1.2 Exercise 1B: DCC from Full-Power Steady-State

Exercise 1B uses the results of Exercise 1A as initial conditions and allows for comparison with just a few simple boundary conditions. The coolant flow rate coasts down linearly from 1.0 to 0.0 kg/s over 1 second. The system depressurizes from 0.7 to 0.1 MPa linearly over 20 seconds. Flow rates in the cavity and the RCCS do not change. The power versus time curve here is based on the 1994 American Nuclear Society decay heat standard. The specific values of power versus time are seen in Table 4. If participants have the option to do so, they should interpolate power linearly between time steps. This problem should be solved with transient solution techniques.

Table 4: Power versus time for Exercise 1B.

Time (s)	Power (W)	Time (s)	Power (W)	Time (s)	Power (W)	Time (s)	Power (W)
0	2200000	150	61160	4000	26576	4000000	3058
0.01	124256	200	57882	6000	23364	5000000	2838
1.5	120868	400	50644	8000	21450		
2	118030	600	46486	10000	20152		
4	109934	800	43428	15000	17886		
6	104566	1000	41030	20000	16104		
8	100584	1500	36564	40000	12958		
10	97460	2000	33418	60000	11418		
15	91784	4000	26576	80000	10428		
20	87802	6000	23364	100000	9724		
40	78342	8000	21450	500000	5852		
60	72864	10000	20152	1000000	4708		
80	69036	15000	17886	2000000	3784		
100	66132	20000	16104	3000000	3344		

3.1.3 Exercise 1C: DCC with PG-29-like Boundary Conditions

The boundary conditions for this sub-exercise are very detailed. Prior to providing the boundary conditions, a common geometry must be established. Participants may set up their geometry as they wish, but for the sake of initial conditions in Exercise 1, the geometry in is used. For example, from $r = 0$ to $r = 0.075$ at a given axial location, the temperature is the same everywhere.

The initial conditions for the helium coolant temperatures can be seen as Table 5. Empty locations in the table indicated regions that should have no primary coolant in them. The initial flow rate everywhere is 0.0 kg/s, and the initial pressure everywhere is 2.076 kPa.

Table 5: Helium initial conditions.

Bottom Elevation/Outer Radius (m)	0.075	0.165	0.177	0.288	0.37	0.473	0.508	0.576	0.604	0.762	0.83185
5.39682											
3.69697											
2.86512		376.3		376.3	376.3	376.3		376.3			376.3
2.48412		376.3		373	373	372.8		376.3			362.1
2.286		376.3		415.3	408.7	386.6		376.3			362.1
2.08788		376.3		415.3	408.7	386.6		376.3			362.1
1.88976		376.3		510.5	608	525.1		376.3			362.1
1.69164		376.3		510.5	608	525.1		376.3			362.1
1.49352		376.3		611.2	568	510.5		376.3			362.1
1.2954		376.3		611.2	568	510.5		376.3			362.1
1.09728		376.3		505.1	642.1	585.1		376.3			362.1
0.89916		376.3		505.1	642.1	585.1		376.3			362.1
0.70104		376.3		730	589.7	579.3		376.3			362.1
0.50292		376.3		730	589.7	579.3		376.3			362.1
0	376.3	376.3	376.3	730	623	503.9	376.3	376.3	376.3		362.1
-0.2225	522.3	522.3	522.3	522.3	522.3	522.3	522.3	522.3	522.3		357.2
-0.55007	357.2	357.2	357.2	357.2	357.2	357.2	357.2	357.2	357.2		357.2
-1.90237	357.2	357.2	357.2	357.2	357.2	357.2	357.2	357.2	357.2		357.2

The temperatures of the solid structures are defined similarly to the initial helium temperatures. Those initial conditions can be seen in Table 6. Heater rod initial temperatures are defined in Table 7. The heating in PG-29 was azimuthally asymmetric. Consequently, the temperatures in HTTF on July 24, 2019 at 3:15:20 p.m. were azimuthally asymmetric too, but for the sake of the code-to-code comparison, the initial temperatures are defined as azimuthally identical. These values are the average of the values around the core.

Table 6: Solid structure initial temperatures.

Bottom Elevation/Outer Radius (m)	0.075	0.165	0.177	0.288	0.37	0.473	0.508	0.576	0.604	0.751	0.762
5.39682											
3.69697	346.1	346.1	346.1	346.1	346.1	346.1	346.1	346.1	346.1	346.1	346.1
2.86512	346.1	346.1	346.1	346.1	346.1	346.1	346.1	346.1	346.1	346.1	346.1
2.48412	376.7	314.6	371.3	373.1	371.3	372.3	373.8	373.8	373.8	378.5	423.2
2.286	388.5	314.6	396.1	426.3	404.8	387.1	373.8	373.8	373.8	386.8	423.2
2.08788	412	314.6	396.1	426.3	404.8	387.1	385.7	373.8	373.8	412.2	423.2
1.88976	461.5	314.6	483.3	507.4	502.7	544.7	385.7	373.8	373.8	412.2	423.2
1.69164	461.5	314.6	483.3	507.4	502.7	544.7	438.8	373.8	373.8	433.5	423.2
1.49352	461.5	314.6	314.5	507.4	562.6	557.2	438.8	373.8	373.8	433.5	423.2
1.2954	505	314.6	314.5	507.4	562.6	557.2	488.9	373.8	373.8	445.1	423.2
1.09728	505	311.3	313.5	789.6	628.3	557.2	488.9	373.8	373.8	445.1	423.2
0.89916	505	311.3	313.5	789.6	628.3	557.2	505.8	373.8	373.8	392	423.2
0.70104	692.4	311.3	789.3	1004.4	589	601.8	505.8	373.8	373.8	392	423.2
0.50292	692.4	311.3	789.3	1004.4	589	601.8	410	373.8	373.8	392	423.2
0	655.2	311.3	789.3	1004.4	589	601.8	410	373.8	373.8	392	357.1
-0.2225	460	460	460	460	460	460	460	460	460	460	357.1
-0.55007	327.4	327.4	327.4	327.4	327.4	327.4	327.4	327.4	327.4	327.4	327.4
-1.90237	477.2	477.2	477.2	477.2	477.2	477.2	477.2	477.2	477.2	477.2	477.2

Table 7: Heater rod initial temperatures

Bottom Elevation/Outer Radius (m)	0.075	0.165	0.177	0.288	0.37	0.473	0.508	0.576	0.604	0.751	0.762
5.39682											
3.69697											
2.86512											
2.48412											
2.286				379.7	667.3	378.8					
2.08788				379.7	667.3	378.8					
1.88976				515.1	667.3	460.5					
1.69164				515.1	667.3	460.5					
1.49352				410.8	544.3	475.6					
1.2954				410.8	544.3	475.6					
1.09728				776.1	314.5	503.2					
0.89916				776.1	314.5	503.2					
0.70104				537.5	314.5	570.7					
0.50292				537.5	314.5	570.7					
0											
-0.2225											
-0.55007											
-1.90237											

All water in the RCCS is initialized at 300 K and a pressure of 0.1 MPa, and RCCS solid components should be initialized at 298.2 K.

This exercise uses measured data from PG-29 to inform the boundary conditions. The measured values were smoothed using a procedure described in Reference [4]. The primary coolant mass flow rate was set at 15 grams per second from 0.0 seconds until 28,800 seconds. At 28,800.5 seconds, the coolant flow rate was set to zero. Coolant flow should be linearly interpolated between 28,800 and 28,800.5 seconds. The helium inlet temperature boundary conditions can be seen in Table 8. The outlet pressure boundary condition can be seen in Table 9.

Table 8: Coolant inlet temperature boundary condition.

Time (s)	Inlet Temp. (K)	Time (s)	Inlet Temp. (K)	Time (s)	Inlet Temp. (K)	Time (s)	Inlet Temp. (K)
0	360.30	32065.5	354.18	59855.5	328.48	91179	317.20
900.5	360.30	33949.5	351.36	61134.5	327.82	91921	317.04
2137.5	360.36	34203	351.00	61993	327.36	94059	316.64
2840.5	358.43	34849.5	350.13	64131	326.31	94169	316.62
4275	356.42	35974.5	348.66	66268.5	325.30	96196.5	316.22
6413	360.36	36341	348.19	66893.5	324.99	96844.5	316.10
8216	361.34	38478.5	345.56	68406.5	324.31	97575.5	315.97
8216.5	361.34	38826	345.17	69670.5	323.78	97753.5	315.94
8550.5	361.45	40335.5	343.55	70544	323.41	98334.5	315.83
9116	361.62	40567	343.32	70960.5	323.24	91179	317.20
10633	362.10	40567.5	343.32	72682	322.56	91921	317.04
10688.5	362.12	40616	343.27	72814	322.51	94059	316.64
12826	362.73	42403	341.51	74093.5	322.06	94169	316.62
13644.5	362.80	42403.5	341.51	74467	321.91	96196.5	316.22
14963.5	362.03	42754	341.18	74509.5	321.89	96844.5	316.10
15603.5	360.85	42870.5	341.07	74819.5	321.78	97575.5	315.97
17101.5	362.24	44891.5	339.16	76957	321.06	97753.5	315.94
17688	363.27	46899	337.19	79095	320.36	98334.5	315.83
19239	364.75	47029.5	337.09	81232.5	319.71		
19358.5	364.81	47691	336.57	83370.5	319.12		
19405.5	364.83	49167	335.38	84740.5	318.76		
20949.5	366.03	50203	334.61	84969	318.70		
21377	366.39	51304.5	333.79	85508	318.55		
22434	366.90	53442.5	332.34	85964	318.43		
23514.5	367.15	55580	330.97	86414	318.30		
25652	366.32	56539	330.39	87645.5	318.02		
27373.5	367.15	57718	329.71	87889.5	317.95		
27790	367.49	58323	329.36	88789	317.73		
29927.5	358.84	59816.5	328.50	89783.5	317.50		

Table 9: Outlet pressure boundary condition.

Time (s)	Pressure (Pa)	Time (s)	Pressure (Pa)	Time (s)	Pressure (Pa)	Time (s)	Pressure (Pa)
0	2.08E+05	21062.5	2.10E+05	42529.5	9.93E+04	66293.5	1.08E+05
300.5	2.08E+05	21377	2.10E+05	42754	9.98E+04	66480.5	1.08E+05
1136	2.08E+05	23514.5	2.10E+05	42849.5	9.97E+04	68406.5	1.08E+05
1727	2.07E+05	25390.5	2.11E+05	43137.5	1.00E+05	70544	1.08E+05
1727.5	2.08E+05	25469.5	2.11E+05	44891.5	9.99E+04	72682	1.08E+05
2064	2.08E+05	25652	2.11E+05	47029.5	1.00E+05	74007.5	1.07E+05
2077	2.08E+05	25700.5	2.11E+05	49167	1.01E+05	74819.5	1.08E+05
2137.5	2.07E+05	27790	2.11E+05	51304.5	1.02E+05	76957	1.07E+05
2774	2.08E+05	29419	1.08E+05	51709.5	1.03E+05	77250	1.08E+05
4275	2.08E+05	29927.5	1.06E+05	52407	1.03E+05	79095	1.07E+05
4957.5	2.08E+05	31994.5	1.02E+05	53442.5	1.04E+05	81232.5	1.07E+05
6413	2.08E+05	32015	1.02E+05	54470	1.04E+05	81612.5	1.07E+05
8550.5	2.08E+05	32038	1.03E+05	55580	1.05E+05	83370.5	1.07E+05
9340.5	2.08E+05	32038.5	1.02E+05	56694	1.06E+05	85508	1.07E+05
10688.5	2.08E+05	32065.5	1.02E+05	57290	1.06E+05	87645.5	1.06E+05
11694	2.08E+05	32363	1.01E+05	57718	1.06E+05	88139.5	1.07E+05
12826	2.08E+05	32363.5	1.02E+05	58323	1.07E+05	89783.5	1.06E+05
14963.5	2.08E+05	34203	1.01E+05	59855.5	1.08E+05	91921	1.07E+05
15714	2.09E+05	34661	1.01E+05	60147.5	1.08E+05	94059	1.06E+05
16482.5	2.09E+05	34835	9.98E+04	60738.5	1.08E+05	96196.5	1.06E+05
17101.5	2.09E+05	34835.5	1.01E+05	61032.5	1.08E+05	98334.5	1.06E+05
17222	2.09E+05	35646	1.00E+05	61033	1.08E+05		
19239	2.09E+05	36341	1.00E+05	61993	1.09E+05		
19440	2.09E+05	38478.5	1.00E+05	64131	1.08E+05		
19440.5	2.10E+05	40616	9.98E+04	66268.5	1.09E+05		

As stated previously, heat generation in PG-29 is azimuthally asymmetric. The power is all generated in heater bank 104. The HTTF is divided into primary, secondary, and tertiary sectors. In PG-29, only the primary and tertiary sectors were heated. For the sake of this exercise, the heat is assumed to be generated equally in each of those sectors. Thus, the power boundary condition provided in Table 10 should be divided by two for each of the heat generating sectors.

Table 10: Heater 104 power boundary condition.

Time (s)	Power (W)	Time (s)	Power (W)	Time (s)	Power (W)	Time (s)	Power (W)
0	3.802E+04	30025	4.869E+04	30230.5	4.877E+04	79896.5	4.486E+01
1799.5	3.802E+04	30037.5	4.863E+04	30729.5	4.896E+04	81945	4.710E+01
1800	3.802E+04	30038	4.874E+04	30819	4.865E+04	83994	4.693E+00
2048.5	3.841E+04	30038.5	4.862E+04	30819.5	4.865E+04	86042.5	0.000E+00
4097	3.989E+04	30040	4.845E+04	32778	4.907E+04	88091	0.000E+00
6145.5	4.120E+04	30040.5	4.860E+04	34826.5	4.887E+04	90139.5	0.000E+00
8194.5	4.071E+04	30042.5	4.860E+04	36875	4.870E+04	92188.5	0.000E+00
10243	4.262E+04	30043.5	4.854E+04	38924	4.839E+04	94237	0.000E+00
12291.5	4.339E+04	30049	4.837E+04	40972.5	4.809E+04	96285.5	0.000E+00
14340	4.518E+04	30050	4.851E+04	43021	4.800E+04	98334.5	0.000E+00
16389	4.570E+04	30062	4.819E+04	45069.5	4.748E+04	79896.5	4.486E+01
18437.5	4.531E+04	30068.5	4.838E+04	47118.5	4.725E+04	81945	4.710E+01
20486	4.525E+04	30069	4.834E+04	49167	4.714E+04	83994	4.693E+00
22534.5	4.434E+04	30072.5	4.838E+04	51215.5	4.669E+04	86042.5	0.000E+00
24583.5	4.418E+04	30081	4.876E+04	53264.5	4.662E+04	88091	0.000E+00
26632	4.403E+04	30112.5	4.854E+04	55313	4.623E+04	90139.5	0.000E+00
28680.5	4.389E+04	30113.5	4.849E+04	57361.5	4.622E+04	92188.5	0.000E+00
28819	4.437E+04	30115.5	4.838E+04	59410	4.613E+04	94237	0.000E+00
28819.5	4.438E+04	30116	4.851E+04	61459	4.558E+04	96285.5	0.000E+00
28874	4.493E+04	30117	4.860E+04	63507.5	2.142E+01	98334.5	0.000E+00
28874.5	4.531E+04	30118	4.850E+04	65556	3.310E+01		
28875.5	4.677E+04	30119	4.857E+04	67604.5	4.087E+01		
28876	4.709E+04	30119.5	4.845E+04	69653.5	4.975E+01		
28876.5	4.694E+04	30120	4.857E+04	71702	5.115E+01		
28903.5	4.782E+04	30121	4.837E+04	73750.5	4.482E+01		
28904.5	4.813E+04	30121.5	4.836E+04	75799.5	4.870E+01		
28959	4.808E+04	30123.5	4.857E+04	77848	4.757E+01		

The presence of coolant channels in the HTTF blocks degrades their thermal conductivity. Some codes may be able to account for this effect inherently, but others cannot. In this sub-exercise, participants should use the thermal conductivity data in Table 11 for the aluminum-oxide core ceramic block (inner reflector, heated regions, and outer reflector).

Table 11: Thermal conductivity data for PG-29 Exercise 1C.

Temperature (K)	Block thermal conductivity (W/m-K)
300	4.2122
400	3.9917
500	1.7037
600	0.5768
700	0.2502
800	0.1569
900	2.78
1000	2.58
1100	2.46
1200	2.40
1300	2.37
1400	2.33
1500	2.27
1600	2.15
1700	1.95
1800	1.63
1900	1.17
2000	0.54

The RCCS is defined by inlet temperature and coolant flow rate boundary conditions that can be found in Table 12 and Table 13, respectively.

Table 12: RCCS inlet temperature boundary conditions.

Time (s)	RCCS Inlet Temp (K)	Time (s)	RCCS Inlet Temp (K)	Time (s)	RCCS Inlet Temp (K)
0	313.53	31724.5	316.17	66268.5	317.27
1873	313.77	32065.5	316.23	68406.5	317.40
1873.5	313.77	34203	316.51	68860	317.44
1874	313.76	36341	316.67	70544	317.54
1874.5	313.76	38461.5	316.76	71490	317.58
1875	313.75	38478.5	316.76	72682	317.66
1875.5	313.75	39273.5	316.78	74819.5	317.83
1876	313.75	39593	316.79	76490.5	317.98
2137.5	313.82	40493	316.80	76957	318.03
2773	309.30	40616	316.80	79095	318.20
2773.5	309.30	41121	316.80	79877.5	318.29
2774	309.30	42259	316.81	80552.5	318.33
2774.5	309.30	42754	316.81	81232.5	318.41
2775	309.30	44891.5	316.79	81647.5	318.46
2775.5	309.29	45344.5	316.78	81703.5	318.46
2776	309.29	47029.5	316.76	83370.5	318.66
3040	306.71	47275.5	316.75	85368.5	318.18
4275	308.43	49167	316.74	85508	318.10
4851	309.09	50145.5	316.74	86955.5	317.82
6413	310.49	50176	316.74	87645.5	317.78
8550.5	311.98	50588.5	316.74	88031	317.75
10688.5	313.11	51304.5	316.74	89783.5	317.63
11968.5	313.66	53442.5	316.77	91921	317.50
12826	313.97	55112	316.80	92879	317.45
14806.5	314.47	55580	316.82	94059	317.38
14963.5	314.03	56304	316.84	95904	317.27
17101.5	313.34	57446	316.88	96196.5	317.26
19239	314.22	57718	316.89	98334.5	317.13
21377	314.92	59855.5	316.98		
23514.5	315.51	59913	316.98		
25652	315.13	59913.5	316.98		
27790	315.06	61993	317.10		
28452	315.31	64131	317.17		
29927.5	315.76	66037	317.26		

Table 13: RCCS flow rate boundary conditions.

Time (s)	RCCS Flow (kg/s)	Time (s)	RCCS Flow (kg/s)	Time (s)	RCCS Flow (kg/s)
0	0.385594	19239	0.384709	79095	0.389894
899.5	0.385594	21377	0.385548	81232.5	0.39033
900	0.385594	23514.5	0.385874	83370.5	0.390559
1783.5	0.380901	24723.5	0.38593	84132	0.390368
1867	0.374159	24825	0.379955	84132.5	0.390322
1867.5	0.374156	24825.5	0.37994	84133	0.390249
1868.5	0.374141	24838.5	0.379514	84133.5	0.390215
1869.5	0.374101	25652	0.369759	84134	0.390189
1870	0.374057	25725	0.374324	84139	0.389722
1870.5	0.374026	25725.5	0.374336	84143.5	0.388957
1873	0.373931	25738.5	0.374692	84144	0.388832
1873.5	0.37397	25739	0.374701	84145	0.388549
1874	0.373997	27790	0.382035	84145.5	0.388379
1874.5	0.37401	29927.5	0.385088	84146	0.388201
2137.5	0.374738	32065.5	0.385585	84146.5	0.387983
2593.5	0.369667	34203	0.385972	85030.5	0
2675.5	0.373831	36341	0.386014	85031	0
2683.5	0.374455	38478.5	0.386338		
2767.5	0.381574	40616	0.386785		
2768.5	0.381594	42754	0.387165		
2769.5	0.381635	44891.5	0.387162		
2770	0.381682	47029.5	0.387109		
2770.5	0.381716	49167	0.387372		
2773.5	0.381787	51304.5	0.387438		
2774	0.381762	53442.5	0.387828		
2774.5	0.381751	55580	0.387533		
4275	0.380357	57718	0.387889		
6413	0.380904	59855.5	0.388407		
8550.5	0.38215	61993	0.389275		
10688.5	0.382987	64131	0.389386		
12826	0.384229	66268.5	0.389798		
14056.5	0.384795	68406.5	0.389694		
14210.5	0.375853	70544	0.389983		
14963.5	0.364352	72682	0.390307		
15110.5	0.372643	74819.5	0.390088		
17101.5	0.381976	76957	0.390089		

Participants should interpolate linearly between boundary conditions. This problem should be solved with transient solution techniques.

3.2 Open Boundary Conditions (Best-Estimate Modeling and Validation)

In Exercise 2, participants are encouraged to test the capabilities of their codes and use their best judgement to develop a best-estimate solution. Participants may wish to perform their own thermal conductivity calibrations, develop initial conditions that include azimuthal asymmetry, or estimate their own flow rates. These are only a few parameters that participants may choose to fine-tune to provide best-estimate solutions. The boundary conditions from Exercise 1 were generated with temperature agreement in mind, but little attention was paid to pressures or pressure drops. Participants may wish to model as much of the HTTF as possible during this exercise and demonstrate agreement with measured data in the primary or secondary loops. The following instruments did not function during the test:

- TS-1301
- TS-1401 (backup to TS-1301)
- TS-1302
- TS-1316 (backup to TS-1302)
- TS-1502
- TS-1516 (backup to TS-1502)
- TS-1503
- TS-1517 (backup to TS-1503)
- TS-1531 (backup to TS-1503)
- TS-1115
- TS-1304
- TS-1305
- TS-1511
- TS-1911
- TF-8205.

It should be noted that instruments CT-1062 and VT-1062 indicate current and voltage flowing through them, but heater 106 was not used as part of the experiment. Due to the azimuthally asymmetric nature of this experiment, it is recommended that participants focus their attention on core blocks 3, 5, and 7, which are the only elevations to have thermocouples in all three sectors of the core.

3.3 Error Scaling (Validation Extrapolation)

The objective of the error scaling exercise is to identify relationships between error and uncertainty in HTTF and error and uncertainty in the reference mHTGR-350. Exercise 2 provides an opportunity for validating systems codes against the HTTF data, but the question remains: how well can models validated based on a low-power, low-flow system like HTTF be said to represent a high-power, high-flow system like the mHTGR-350. Exercise 3 provides an opportunity to bound that validation extrapolation. In the systems-code exercises, participants can use systems codes models they develop for the mHTGR-350, but we also provide some reference values here so that users may perform error scaling without also needing to solve the mHTGR-350 benchmark. We have taken existing DCC models in the mHTGR-350 and performed sensitivity studies on them to provide sensitivity coefficients for error scaling.

The DCC in the mHTGR-350 occurs from full-power steady state. The coolant flow rate drops linearly from 157.0 kg/s to 0.0 kg/s over 20 seconds, and depressurization (from 6.39 to 0.1 MPa) occurs linearly over the same period. SCRAM occurs at 27 seconds. This is a fixed SCRAM time rather than an actuation of some hypothetical reactor protection system. The decay heat is defined at several axial and radial locations based on an assumed power history. The mHTGR-350 benchmark model has been modified to use the thermal conductivity of unirradiated graphite in the fueled regions of the core.

The sensitivity study perturbs the variables listed in Table 14 according to normal distributions described by the mean and standard deviations listed in the table. Multipliers on thermophysical properties were applied to each value in the temperature-dependent thermal conductivity. Each value was given the same multiplier at the same time. For example, if the thermal conductivity multiplier was 1.5, the thermal conductivity at each temperature was multiplied by 1.5 rather than using a unique multiplier for each temperature. The decay heat multiplier was applied to the decay heat at each location in the core.

Table 14: mHTGR-350 sensitivity study parameter distributions.

Parameter	Mean	Standard Deviation
Inlet Temperature (K)	532.0	2.142
Coolant Flow Rate (kg/s)	157.0	1.127
Block Thermal Conductivity Multiplier	1.0	0.3
Block Heat Capacity Multipliers	1.0	0.15
Fuel Thermal Conductivity Multiplier	1.0	0.1
Fuel Heat Capacity Multiplier	1.0	0.1
Friction Multiplier	1.5	0.1667
HTC Multiplier	1.0	0.15
Decay Heat Multiplier	1.0	0.035
Coast-down Time (s)	25	5
SCRAM Time (s)	42	15

The figures of merit for this sensitivity study are instantaneous peak fuel temperature, instantaneous coolant outlet temperature, maximum fuel temperature over the entire transient, and maximum coolant outlet temperature over the transient. We present reference sensitivity coefficients in Table 15. Sensitivity coefficients are computed via linear regression and non-dimensionalized according to the equation below, where S is a sensitivity coefficient, L is the linear regression coefficient, X is the input in question, and Y is a figure of merit.

$$S = L \times \frac{\bar{X}}{\bar{Y}}$$

Table 15: DCC sensitivity coefficients.

Parameter	Maximum Block Temperature Sensitivity Coefficient (-)	Maximum Outlet Temperature Sensitivity Coefficient (-)
Inlet Temperature (K)	0.484	0.537
Coolant Flow Rate (kg/s)	0.039	0.012
Block Thermal Conductivity Multiplier	-0.011	0.0
Block Heat Capacity Multipliers	-0.040	0.0
Fuel Thermal Conductivity Multiplier	-0.004	0.0
Fuel Heat Capacity Multiplier	-0.009	0.0
Friction Multiplier	-0.005	0.0
HTC Multiplier	-0.005	-0.009
Decay Heat Multiplier	0.008	-0.002
Coast-down Time (s)	-0.018	0.006
SCRAM Time (s)	0.078	0.0

Participants are encouraged to use error scaling techniques such as dynamical system scaling, representativity, or others, to conduct their error scaling calculations. We provide the reference mHTGR-350 sensitivity coefficients for participants who do not have access to an mHTGR-350 model. Participants who have access to an mHTGR-350 model are free to conduct their own sensitivity analysis for their error scaling studies.

4. Conclusions

The collaboration is underway between INL, OSU, ANL, and CNL to develop specifications for an HTGR thermal hydraulics benchmark based on HTTF experiments. The HTTF benchmark will be a single-physics benchmark that provides the opportunity for code-to-code and code-to data comparisons. The benchmark consists of problems for lower plenum mixing, DCC, and PCC experiments. Each problem is divided into three phases: fixed boundary conditions, best-estimate boundary conditions, and error scaling. This report has presented a draft of the specifications for the DCC problem, whose development is led by INL. The lower plenum mixing problem is being led by OSU, and the PCC is being led by ANL. The benchmark as a whole is led by INL under the auspices of the ART program. This benchmark will provide an important opportunity for both code-to-code verification studies and validation studies against measured data for HTGR thermal hydraulics modeling tools.

5. References

[1] Ortensi, J., G. Strydom, S. Sen, V. Seker, K. Ivanov, I. Clifford, J. Hou, H. C. Lee, N. Tak, T. Y. Han, H. J. Shim, U. Rohde, E. Fridman, Bilodid, A. Seubert., "Prismatic coulped netronics/thermal fluids transient benchmark of the MHTGR-350 MW core design: benchmark definition," Organization for Economic Cooperation and Development - Nuclear Energy Agence, Paris, 2018.

[2] Gutowska, I., B. Wood, "OSU High Temperature Test Facility Design Technical Report, Revision 2," Oregon State University, Ocrvallis, OR 2019.

[3] Bayless, P. "RELAP5-3D Input Model for the High Temperature Test Facility," Idaho National Laboratory, Idaho Falls, ID, 2018.

[4] Epiney, A, "RELAP5-3D Modeling of High Temperature Test Facility Test PG-26," Idaho National Laboratory, Idaho Falls, ID, 2020

[5] Naknikian-Weintraub, B., U. Babineau, B. Woods, "OSU High Temperature Test Facility Test Acceptance Report: PG-29 Low Power (<350 kW) Double Ended Inlet-Outlet Crossover Duct Break Hybrid Heater," Oregon State University, 2019.